Timing of strain partitioning and magmatism in the Scottish Scandian collision, evidence from the high Ba-Sr Orkney granite complex

Anders Mattias Lundmark[1], Lars Eivind Augland[2] and Audun Dalene Bjerga[1]

[1]University of Oslo, Department of Geosciences, PO Box_ 1047 Blindern, 0316 Oslo, Norway

[2]University of Oslo, Centre for Earth Evolution and Dynamics (CEED), PO Box 1028 Blindern, 0315 Oslo, Norway

Supplementary material: Geochronological and geochemical data as spreadsheets are available at https://doi.org/10.1144/sjg2018-001

Abstract

The Orkney granite complex dominates the outcropping basement on Orkney, Scotland. It comprises a grey and a pink variably foliated granite, and structurally younger pegmatites and aplites. Based on geochemical characteristics the granites are assigned to the Scottish high Ba-Sr granites. The granites are deformed by synmagmatic extensional east-west trending mylonite zones. These are locally overprinted by similarly oriented extensional phyllonites, and in one case by similarly oriented extensional faults. The grey and the pink granites are dated by zircon U-Pb CA-ID-TIMS to 431.93 ± 0.46 Ma and 430.26 ± 0.92 Ma, respectively. An aplite cutting mylonitic granite and cut by phyllonite is dated to 428.50 ± 0.31 Ma. We interpret the shear zones to record north-south extension during emplacement and cooling of the granites, likely at a shallow crustal depth (4-12 km). The extension is best explained by a subsidiary pull-apart structure related to displacement on the Great Glen Fault. In this case, the Orkney granite complex dates transcurrent faulting to 432-429 Ma, coeval with the 431-429 Ma Moine thrust. This indicates that strain partitioning and high Ba-Sr magmatism across the Scottish highlands was an immediate response to attempted subduction of Avalonia beneath Laurentia during the Scandian collision.

Introduction

The Scandian collision was the culmination of the Caledonian orogeny, as the newly amalgamated Avalonia and Baltica collided with Laurentia in the Wenlock (433.4-427.4 Ma; timescale of Cohen et al. 2013, updated in 2017) to form the supercontinent Laurussia. In Scotland, the Laurentian margin (consisting of the Hebridean terrane, the Northern and the Grampian Highlands terranes), a Paleozoic island arc (the Midland Valley terrane) and an accretionary prism (the Southern Uplands terrane) were compressed and reshaped by thrusting and crustal scale strike-slip faults as they collided with the northern edge of Eastern Avalonia (Legget et al. 1979; Bluck 1983; Soper et al. 1988). Syn- to post-collisional magmatism, ranging from ultramafic to granitic (the Newer granites), was channeled through, and emplaced along, shear zones and accompanied by local metamorphism (e.g. Watson 1984; Robinson et al. 1988; Jacques and Reavy 1994; Dewey and Strachan 2003). Atherton and Ghani (2002) proposed that the Scandian collision was accompanied by slab breakoff, providing a new framework for our understanding of the orogeny. This model has subsequently been modified and developed by e.g. Neilson et al. (2009) and Miles et al. (2016). Key inputs for this model have been the nature and timing of magmatism and deformation. A particularly fruitful approach has been to combine compositional, structural and age data from the Newer granites to constrain both the deep processes that led to the 430

– 380 Ma Newer granite magmatism, the structural setting during their emplacement, and the precise ages of these events (e.g. Kocks et al. 2013; Miles et al. 2016).

Here we report new compositional, structural and high precision age data from the little studied Caledonian basement on the Orkney Islands. The data resolve outstanding questions regarding the Orkney basement, and yield new constraints on the timing and nature of early Scandian deformation and high Ba-Sr magmatism in Scotland, and hence on permissible models for the Caledonian tectonomagmatic evolution.

Geological background

The ca. 500-390 Ma Caledonian orogeny encompasses the amalgamation of Avalonia, Baltica and Laurentia through the subduction of the intervening Iapetus Ocean, leading to the formation of Laurussia (McKerrow et al. 2000). The Caledonian orogeny includes several orogenic events. Subduction of the Iapetus Ocean along the eastern margin of Laurentia led to accretion of microcontinents, island arcs and oceanic crust during the 495-450 Ma Taconian orogeny in Newfoundland (van Staal et al. 2007; van Staal and Hatcher 2010). In Scotland, the 475-465 Ma Grampian orogeny, welding the Grampian Highlands terrane to the Midland Valley island arc (Fig. 1; Chew and Strachan 2014), is regarded as one distinct event in this diachronous accretionary belt along the Laurentian margin (Friedrich et al. 1999; Soper et al. 1999; Oliver 2001). One consequence of the collision was crustal melting and emplacement of ca. 470 Ma S-type granites in the Scottish Northern and Grampian Highlands (part of the pre-Scandian Caledonian granites; Oliver et al. 2008). On the opposite side of the Iapetus Ocean, Avalonia and Baltica underwent late Ordovician - early Silurian soft docking as the Tornquist Sea (an arm of the Iapetus Ocean) subducted beneath the eastern margin of Avalonia (Soper and Woodcock 1990; Torsvik and Rehnström 2003). Continued subduction of the Iapetus Ocean beneath Laurentia led to the formation of an accretionary prism (the Southern Uplands) along the Grampian margin (Legget et al. 1979; Stone 2014), and ultimately to collision between the amalgamated Avalonia-Baltica block and Laurentia at ca. 430 Ma (Kinney et al. 2003), commonly referred to as the Scandian collision (Stephens and Gee 1989). Whereas the collision between Baltica proper and Laurentia led to deep subduction of the leading edge of Baltica beneath Laurentia (e.g. Andersen et al. 1991), the juxtaposition of the Scottish Grampian orogen and Avalonia across the Southern Uplands accretionary prism was less forceful (Dewey and Strachan 2003). The Scandian collision was oblique (Torsvik et al. 1996), and in Scotland large scale thrusting, e.g. across the Moine thrust, was accompanied by crustal scale sinistral strike slip faulting, e.g. along the Great Glen-Walls Boundary faults (Soper et al. 1992). The collision marked the start of granitic magmatism, the Newer granites (Read 1961), throughout the British Isles (Miles et al. 2016). Many of these granites are emplaced along thrust or strike-slip faults (Dewey and Strachan 2003, and references therein).

To account for Scandian deformation in the Northern Highlands terrane, and its absence in the Grampian Highlands terrane, a sinistral displacement of ≥700 km on the Great Glen Fault and related structures has been proposed in order to position the Grampian Highlands terrane outside the zone of Scandian deformation (Fig. 1; Soper et al. 1992; Dewey and Strachan 2003). It has been speculated that these sinistral shear zones form part of an orogen-scale shear system that linked up with terrane bounding faults on Svalbard (Harland et al. 1992; Soper et al. 1992). The Scottish terranes discussed above continue westwards to resurface on Ireland (Chew and Strachan 2014), and eastwards into the North Sea (Lundmark et al. 2014). Hence, the Orkney Islands and Shetland west of the Walls Boundary Fault are regarded as the north-eastern continuation of the Northern Highlands terrane, whereas Shetland east of the Walls Boundary Fault is interpreted as the continuation of the Grampian Highlands (McBride and England 1999).

From ca. 410 Ma the Caledonian orogen underwent regional extensional collapse (Dewey and Strachan 2003), possibly in response to the Variscan orogeny to the south (Chauvet and Séranne 1994;

Rey et al. 1997; Fossen 2010). In north-eastern Scotland the extension led to the formation of the Devonian Orcadian basin. Presently, Old Red Sandstone laid down in the Orcadian basin is exposed along the coast of northeastern Scotland and on the Orkney Islands and Shetland. On Orkney, sparse inliers of basement are exposed amid the Devonian sediments (Mykura et al. 1976); this basement is the focus of the present investigation.

Previous work on the basement of the Orkney Islands

Mykura et al. (1976) compiled a brief description of the Orkney basement, partly based on earlier descriptions by Steavenson (1928) and Wilson et al. (1935; cited in Mykura et al. 1976). He described the basement as dominated by coarse grey and pink poorly foliated granites, locally grading into granitic gneiss in some of the southern exposures (presumably referring to southern Mainland around Stromness, and on the northern shore of Graemsay; Fig. 2a). Based on the locally intense deformation he proposed that the granites most likely form part of the Scottish pre-Scandian Caledonian granites. Mykura et al. described several different types of schists found as xenoliths in the granites, locally forming blocks up to several 100's of metres across. The granites and the schists are both cut by late granitic pegmatite and pink aplite.

In a 2003 paper on the Orkney basement Strachan provides the first modern structural investigation of the rocks. He describes strongly foliated meta-granites, locally grading into augen gneiss, which he suggests may form intrusive sheets with thicknesses in the order of 100's of metres. Contacts with larger masses of schist are interpreted as contacts with in situ country rock belonging to the Moine schists (with the development of the schistosity referred to as "D1"). Strachan suggests that the foliation in the meta-granites and the country rock is typically concordant or near concordant. The fabrics in the meta-granites are suggested to represent lower amphibolite facies recrystallization related to a deformational event taking place either during or after granite emplacement ("D2"). A final deformation event ("D3") is suggested from map-scale changes in strike and dip of the granite fabric (cf. Fig. 2), interpreted to reflect gentle, north trending upright folds plunging gently to the south. The granites and the schists are cut by late, undeformed (with some exceptions) granitic and aplitic veins (of uncertain relation to D3). The regional context coupled with petrological and structural considerations prompted Strachan to correlate the Orkney granites with the Scottish Newer granites, and in particular with the typically gently inclined, concordant granite sheets emplaced during Scandian thrusting in Scotland (e.g. Kinny et al. 2003; Kocks et al. 2006). These early Scandian syn-thrusting granites contrast with the younger steep-sided composite Rogart pluton that exemplifies emplacement during strike-slip movement (Kocks et al. 2013).

Field observations

Basement outcrops in the Orkneys are restricted to two main areas on Mainland Orkney, around the town of Stromness in the south and at Yesnaby in the west, and to one area along the northern shore of the small island of Graemsay (Fig. 2a). Apart from the excellent outcrops along the coastal sections, basement exposures are generally small and patchy in the hilly landscape around Stromness and inland of the Yesnaby coastal outcrop. The basement is overlain by mid- to upper Devonian sedimentary rocks of the Middle Old Red Sandstone, with one instance of potential Lower Old Red Sandstone cropping out near Yesnaby (the Yesnaby Sandstone Group; Mykura et al. 1976).

The Orkney granite complex

The dominant lithology of the basement is, as previously described by Mykura et al. (1976) and Strachan (2003), variably foliated granite. Two main phases of granite can be recognised in the field and in thin sections; a grey to variably purplish or pinkish, generally coarse grained biotite granite, and a pink, in-equigranular biotite granite with variable but typically medium to coarse grain size and large, up to 2 cm alkali feldspar crystals (Fig. 3). The grey granite contains ca. 35% plagioclase, 25% alkali feldspar, 25% quartz, up to 15 % biotite and up to 2% oxides (monzo-granite sensu Streckeisen 1974). Apatite and zircon are commonly observed as accessory minerals. The pink granite comprises ca. 40% to 45% alkali feldspar, 40 % quartz, 10 to 15 % plagioclase and up to ca. 5 % biotite and some oxides (syeno-granite sensu Streckeisen 1974). The colour difference between the two granite types mainly reflects the relative proportions of alkali feldspar and plagioclase. Feldspars in both granites have been variably sausseritised and sericitised. The pink granite invariably intrudes the grey granite and is hence structurally younger. In both granites there is ample evidence for high temperature recrystallization, such as lobate grain boundaries between quartz grains and between quartz and feldspar grains, subgrain formation in feldspars and myrmekite growth in feldspars. These textures are locally overprinted by lower temperature textures such as subgrain formation in quartz and core mantle textures in feldspars.

Partly migmatised paragneisses occur as xenoliths in the granites. They are increasingly common towards the south-western part of the Stromness outcrop, suggesting that this represents a marginal part of the granitic complex. Whether the apparently contiguous paragneiss cropping out along the shore southwest of Stromness represents the country rocks to the granites as suggested by Strachan (2003) or mega-xenoliths as suggested by Mykura et al. (1976) is not clear, as only a few tens of metres of basement is exposed. At Yesnaby, xenoliths of paragneisses increase in frequency towards the northwest of the outcrop, with a potential contact to the country rock exposed along the north-western shore. Both the grey and the pink granite are intruded by numerous granitic pegmatites and aplites.

Deformation zones: proto-mylonites and mylonites

The Orkney granite complex is cut by east-west striking shear zones that include mylonites at the three main sites of basement outcrops, i.e., in Stromness, on Graemsay and at Yesnaby (Fig. 2, 3). In Stromness and on Graemsay east-west striking shear zones are exposed along the shores, and locally develop into mylonites, which are south-dipping and only a few metres thick (Fig. 3a). Only short sections of the mylonite zones are exposed along the shore lines at these two locations, in the order of a few metres along strike. The foliation in the granites progressively changes orientation towards the shear zones into parallelism with the mylonite foliation. Kinematic indicators and lineations in the mylonites at Stromness and Graemsay indicate a top-to-south extensional sense of shear (Fig. 2b, 3b). These deformation zones presumably equate to "*the highly sheared granites*" in the area reported by Mykura et al. (1976), on which he based his correlation of the Orkney granites with the pre-Scandian Caledonian granites, and the augen gneiss of Strachan (2003), or in the words of Steavenson (1928, p219) "*a rock which is sometimes a granite, sometimes a foliated granite, and sometimes a true gneiss*". In this paper we refer to the shear zones as proto-mylonites, locally grading into mylonites.

The mylonite zone at Yesnaby, on the other hand, is north-dipping and significantly thicker than at Stromness and Graemsay, with a thickness of several 10's of metres exposed between the sea and the overlying Devonian sediments. Exposure along strike is in the order of 100 metres. Kinematic indicators and lineations show a top-to-north extensional sense of shear (Fig. 2b, 3c-e). The mylonite zone mainly cuts across the granites, but anastomosing strands of the mylonite also cut across the paragneisses along the contact between granite and paragneisses (Fig. 3f). Individual veins of granite can locally be seen cutting across parts of the mylonitic fabric, only to be swept into the shear planes of the mylonite further into the mylonite zone. The mylonitic shearing must therefore have taken place while the granites were emplaced. Some granitic pegmatites and aplites display a similar field appearance, and thus appear to be coeval with mylonitisation, but most pegmatites and aplites simply cut the mylonites, demonstrating that minor magmatic activity occurred after ductile displacements on the mylonites (Fig. 3g).

In thin section, quartz grains in the syn-kinematic granite from the Yesnaby mylonite zone have lobate grain boundaries indicating that grain boundary migration took place during deformation. Locally, this texture is overprinted by subgrain rotation recrystallization. The alkali feldspars also show development of subgrains, myrmekite growth and formation of core-mantle textures (White 1975), typically with biotite surrounding the feldspar porphyroclasts (Fig. 3h, i). The preserved deformation textures indicate that the granites initially were deformed at temperatures in excess of 600°C and were overprinted by lower temperature structures (Vidal et al. 1980; Gapais, 1989; Gates and Glover, 1989; Simpson and Wintsch, 1989; Gower and Simpson, 1992; Tribe and D'Lemos, 1996; Stipp et al., 1999; Stipp, 2002).

Since the fabric in the granites was formed during high temperatures and is reoriented by the syn-magmatic mylonite zones, the fabric must have formed as the granites were emplaced, or immediately thereafter.

Deformation zones: phyllonites

The mylonites at Stromness, Graemsay and Yesnaby are all partly overprinted by numerous cm to dm-thick phyllonite shear zones (e.g. Fig. 3j). These have the same orientation and show the same sense of shear as the mylonites they deform (Fig. 2b). The phyllonites are dominated by fine grained quartz, muscovite and chlorite and include fine grained muscovite fish consistent with the macroscopic shear sense indicators (Fig. 3k). The amount of displacement can locally be estimated by using pegmatites and aplites as structural markers; at Yesnaby a pegmatite is progressively displaced by several cm-thick top-to-north phyllonites, each phyllonite contributing in the order of a dm of displacement. Overall, the limited width of phyllonites observed in the field and the small offsets associated with them indicate that the extension was relatively minor. In Stromness, the mylonites and phyllonites are overprinted by kinematically equivalent brittle faults. All these structures testify to north and south directed extension at progressively lower metamorphic conditions, from amphibolite facies (>600 °C) to greenschist facies or lower.

U-Pb CA-ID-TIMS geochronology

Analytical techniques

The sampled rocks were crushed, pulverised and reduced on a Wilfley table before separation of heavy minerals through standard magnetic and heavy liquid techniques at the University of Oslo. Zircons were selected under an optical microscope, annealed for ca. 72 hours at ca. 900°C and chemically abraded with HF at ca. 195°C for 14 hours (Huyskens et al. 2016; Mattinson 2005), or for the most metamict grains of AB16-04, air abraded for ca.12 hours (Krogh 1982). The zircon grains chosen for analyses were spiked with a mixed ^{202}Pb-^{205}Pb-^{235}U tracer that has recently been calibrated to the EARTHTIME (ET) 100 Ma solution (Svensen et al. 2015). After spiking, the zircons were dissolved in HF (+HNO_3) at ca. 195ºC for 5 days (AB16-04, AB and AB 16-05) in Krogh type bombs or for >48 hrs in micro-capsules enclosed in a Parr type bomb (ML17-15). Chemical separation was done for all grains. Details of the mass spectrometric techniques used are presented in detail in previous articles (Augland et al. 2010, with upgraded laboratory parameters: Pb blank generally <1 pg with a composition of ^{206}Pb/^{204}Pb = 18.59 ± 0.77; ^{207}Pb/^{204}Pb = 15.24 ± 0.38; ^{208}Pb/^{204}Pb = 35.8 ± 1.2). The raw data were reduced using Tripoli (Bowring et al. 2011) and analytical errors and corrections were incorporated and propagated using an Excel macro based on published algorithms (Schmitz and Schoene 2007). Ages were calculated using ISOPLOT (Ludwig 2003) and with specified decay constants (Jaffey et al. 1971) and are presented in Table 1 and as a spreadsheet in Appendix 1.

Results

1. Grey Granite (AB16-05): The zircons from this sample have a homogeneous composition and are euhedral, dominated by (100) crystal faces, colourless, core-free grains with some inclusions. Aspect ratios of the grains range from 3 to 5. Four clear, colourless, high aspect-ratio zircons were analysed and yielded concordant and equivalent data (Fig. 4; Table 1) that are used to calculate a weighted mean

$^{206}Pb/^{238}U$ age of 431.93 ± 0.46 Ma (2σ; MSWD = 0.96). As there is no spread beyond individual analytical errors, this age is considered to represent the crystallisation age of the granite.

2. Pink granite (AB16-04): This sample contains both euhedral and subrounded zircons, typically highly metamict and altered. The zircons have a brown-reddish colour and the euhedral grains have aspect ratios ranging from 2 to 5. Due to the metamict character of the grains chemical abrasion tended to dissolve the zircons completely, with the exception of one euhedral medium aspect ratio zircon that gave a concordant age of 430.26 ± 0.92 Ma (2σ; MSWD of concordance = 0.31), and several fragments that are interpreted to represent inherited cores with Proterozoic ages (Fig. 4; Table 1). To test if the concordant age of 430.26 Ma represents the crystallisation age, 3 metamict zircons of the same morphology were air abraded and analysed. These analyses are discordant but collinear and these 3 zircon analyses combined with the concordant chemically abraded zircon yields an upper intercept age of 427 ± 24 Ma (2σ; MSWD = 3.4). This age overlaps well with the concordant age of the chemically abraded zircon of 430.26 ± 0.92 Ma supporting an interpretation of this age as the age of crystallisation of the pink granite.

3. Aplite (ML17-15): The aplite contains both subrounded, clearly xenocrystic grains and a couple of clear, euhedral very high aspect ratio (>1:6) zircons and some fragments that appear to be dominated by (110) crystal faces and stem from high aspect ratio grains. One high aspect ratio grain and five fragments were analysed. Three of the fragments gave Neoproterozoic ages varying from ca. 900 to 720 Ma ($^{207}Pb/^{206}Pb$-ages), whereas the euhedral grain and the two remaining fragments are identical within errors and concordant at ca. 428 Ma. A weighted mean $^{206}Pb/^{238}U$ age of 428.50 ± 0.31 Ma (2σ; MSWD=0.40) of the three analyses (Fig. 4; Table 1) is interpreted as the age of intrusion of the aplite.

4. Inherited zircons: The inherited grains present in the pink granite and the aplite range from Mesoproterozoic to mid-Neoproterozoic in age. These zircons are interpreted to originate from the paragneiss that makes up the country rock to the granites, and is interpreted as Moine metasediments (Strachan 2003). The age range of the inherited zircons analysed here are compatible with this interpretation, as similar detrital zircon ages are typical in the Moine metasediments on the Scottish mainland. Two inherited zircons from the aplite yield ages in the range 720 to 760 Ma, corresponding to the Knoydartian metamorphic events that affected the Moine metasediments from ca. 725 to 840 Ma (e.g. Kirkland et al. 2008; Cawood et al. 2015).

Rock classification and geochemistry

Analytical techniques

Three rock samples each from the grey and pink granite were analysed for major and trace elements. Major elements were determined by whole-rock lithium borate fusion (FUS) and inductively coupled plasma-atomic emission spectrometry (ICP-AES), base metals by four acid digestion and ICP-AES, remaining analysed trace elements were determined by FUS inductively coupled plasma mass spectrometry (ICPMS). The analyses were done as part of the ME-MS81d and ME-4ACD81package at ALS, Piteå, Sweden. The results are shown in Table 2. The data are given as a spreadsheet in Appendix 2.

Results

In the total alkali vs. silica rock classification diagram all analyses plot in the granite field, except for one analysis of the grey granite that plots in the quartz diorite (granodiorite) field (Fig. 5a; Cox et al. 1979). Selected major and trace element data from the granites are shown in Fig. 5b. The data are normalized to primordial mantle after McDonough and Sun (1995). The typical high Ba-Sr signature is exemplified by data from the Migdale granite, which is associated with the Ach'Uaine Hybrid appinites (Fowler and Henney 1996; Fig. 1). The pink and grey granite display similar patterns in the plot, but are distinct due to the typically more enriched and less fractionated character of the grey granite. Both granites lack Eu-anomalies, and exhibit troughs for Nb, Ta, P and Ti.

Average Sr-, Ba- and Rb contents of 870, 1200 and 80 ppm for the grey granite and 370, 1080 and 110 ppm for the pink granite yield typical high Ba-Sr signatures in a ternary Rb-Ba-Sr diagram (Fig. 5c; Tarney and Jones 1994).

Discussion

The relation of the Orkney granite complex to the Scottish Caledonian granites

Based on its field appearance the Orkney granite complex was previously linked to the pre-Scandian Caledonian granites by Mykura et al. (1976), and to the Scandian Newer granites by Strachan (2003). The new age data show that the Orkney granite complex was emplaced during a relatively short time span from ca. 432 to 429 Ma, thus confirming the interpretation of Strachan (2003).

The Newer granites in the Northern and the Grampian Highlands are subdivided into two compositionally distinct suites, the Cairngorm suite and the Argyll, high Ba-Sr suite (Stephens and Halliday 1984; Fig. 1). The Cairngorm suite yields characteristic negative anomalies in Sr (and commonly Ba), Ti and P, coupled with high Rb, Th and U, relatively high Y and HREE relative to Ti, and small negative Nb-anomalies. The Argyll suite, on the other hand, is characterized by high Ba and Sr, low Rb, low Y and HREE, and marked negative Nb anomalies (Tarney and Jones 1994). In Fig. 5b the normalized element signatures of both the grey and the pink granite display the characteristic signature of the high Ba-Sr granites, and the grey granite in particular is strikingly similar to the high Ba-Sr Migdale granite associated with the Ach'Uaine Hybrid Appinites (Fowler and Henney 1996). The Orkney granite complex is therefore assigned to the Argyll suite, and henceforth referred to as a high Ba-Sr granite.

Local setting of the emplacement of the Orkney granite complex

The limited and patchy exposure of the Orkney granite complex allows for different interpretations regarding the shape of the intrusions, the nature of the contacts to surrounding basement rocks and the deformational history (cf. Mykura et al. 1976; Strachan 2003). The main contribution of this paper with regards to field geology is the observation that the granites were emplaced coeval with the formation of extensional mylonitic shear zones. These shear zones are present at all three of the main exposures of the granites (Fig. 2a, b). Dating of the syn-mylonitisation grey and pink granites along with dating of a post-mylonitisation aplite constrains this ductile, broadly north-south extension, and the foliation in the granites, to 432-429 Ma.

Textures in the mylonites indicate shearing at progressively lower temperatures (see description above). Overprinting of the mylonites by cm- to dm-thick extensional phyllonites testifies to continued post-magmatic north-south extension. Since the phyllonites are kinematically equivalent to the mylonites, we interpret the phyllonites as a lower temperature continuation of the syn-magmatic deformation. Given that mylonitisation took place at elevated temperatures associated with the 432-430 Ma main granitic magmatic phase, and ceased prior to emplacement of the aplites at 429 Ma, only to be followed by kinematically equivalent phyllonitisation, we interpret the extensional deformation to have taken place during cooling of the granites to the regional ambient temperature.

Overprinting of mylonitic and pyllonitic shear zones by kinematically equivalent brittle faults along the Stromness beach further suggests that some extension continued under brittle conditions; alternatively, the faults could reflect a later, unrelated extensional episode where faulting was oriented by the ductile/semi-brittle structures in the shear zones. In the former case, the ambient temperature must have been below the brittle – ductile transition. We therefore suggest that the granite complex was emplaced at a shallow crustal level (<12 km). This interpretation is supported by the large number of angular xenoliths observed towards the presumed borders of the granites, consistent with epizonal emplacement. We interpret the locally concordant relation between granites and country rocks (Strachan 2003; Fig. 3f) to reflect an extensional ca. 430 Ma fabric rather than forceful emplacement of the granite complex at depth. The local mylonitisation of felsic gneisses up to a few metres away from the granites at Yesnaby is compatible with contact heating of the country rock (or mega-xenoliths). Sub-volcanic (<4 km) features such as porphyric dykes and miarolitic cavities are not observed in the Orkney granite complex. We therefore propose an emplacement depth of ca. 4-12 km. This constrains the amount of exhumation from 430 to ca. 400 Ma, when Lower and Middle Old Red sediments of the Orcadian basin were deposited on the granites (Mykura et al. 1976).

The Scottish high Ba-Sr granites are commonly associated with ultramafic to intermediate rocks and are regarded as the end-products of assimilation – fractional crystallization processes in mafic mantle-derived melts (e.g. Fowler and Henney 1996). Though this view has been challenged with regards to some high Ba-Sr granites (Neilson et al. 2009), the strong similarities between the Orkney granite complex and the Migdale granite, associated with the Ach'Uaine Hybrid Appinites, suggest that an assimilation-fractionation model is applicable for the Orkney granite complex. This in turn implies that the Orkney granite complex represents the felsic part of an igneous complex of more mafic composition deeper beneath the Orkney Islands.

Regional setting of the emplacement of the Orkney granite complex

Geographically, the Orkney granite complex crops out roughly midway between the offshore continuations of the Great Glen Fault (Flinn 1992) and the Moine thrust (Bird et al. 2015; Fig. 1). Newer granites are associated with both types of settings, i.e. thrusting and strike-slip faulting. Indeed, a temporal evolution has been proposed where early (430-425 Ma) Newer granites are syn-thrusting, and later (<425 Ma) Newer granites typically are associated with strike-slip faulting. Thus, a structural shift from predominantly orogen-normal thrusting to predominantly strike-slip deformation has been proposed to occur at ca. 425 Ma (Dewey and Strachan 2003; Kocks et al. 2013), and is commonly alluded to in the literature (e.g. Atherton and Ghani 2002; Lancaster et al. 2017). Based on the interpretation of compressional structures (D2 and D3) in the Orkney granite complex, Strachan (2003) suggested that the granite complex intruded as (gently inclined) sheets as part of the early, syn-thrusting Newer granites.

The new 432-429 Ma age of the Orkney granite complex makes it coeval with movements along the Moine thrust (Fig. 1). The latter forms part of a foreland propagating, mainly in-sequence fault system that formed in response to Scandian collision (e.g., Kinny et al. 2003; Goodenough et al. 2011). The Moine thrust is characterized by west-north-west directed thrusting and mylonitisation (Holdsworth et al. 2007; Law and Johnson 2010, and references therein). The thrusting has been dated to 431–429 Ma by Goodenough et al. (2011), who determined zircon U-Pb TIMS ages of 430.7 ± 0.5 Ma for pre-/syn-kinematic intrusions, and 429.2 ± 0.5 Ma for post-kinematic intrusions (Loch Borralan and Loch Ailsh Plutons in Fig. 1).

However, in contrast to the Moine thrust, the horst-like geometry formed by the extensional shear zones in the Orkney granite complex (cf. Fig. 2) presumably forms part of a larger extensional graben that created space for the intrusions (i.e., the geometry of the shear zones are incompatible with a pop-up structure and thus require other, unexposed extensional faults to the north and south). This extensional setting appears at odds with an association with west-north-west thrusting farther west at 430 Ma. On the other hand, since the Orkney granite complex crops out nearly 50 km west of the Great Glen Fault it is geometrically unfeasible that it reflects a pull-apart directly associated with a jog or a step along the main fault (cf. Fig. 1). Though the limited outcrops of the Orkney granite complex makes interpretations of the large-scale structure speculative, we present a few possible alternatives that associate the Orkney granite complex with the transcurrent Great Glen Fault and potential subsidiary faults (Fig. 6). Similar settings have been suggested for other Newer granites (e.g. Jacques and Reavy 1994; Dewey and Strachan 2003, and references therein). For example, the stick-point sketch in Fig 6a is adapted from an interpretation of the Clunes granite published by Stewart et al. (2001), the jog on a subsidiary fault parallel to the Great Glen / Leannan fault has been proposed for the Donegal pluton (Fig 6c; Hutton 1982; Arthur 1982), and a jog on an anti-Riedel shear zone has been proposed for the Rogart pluton (Fig 6e; Kocks et al. 2013). These conceptual models do not take into account the potential for strain rotation in a strike slip setting or effects of preexisting basement structures (for examples of the latter, see Jacques and Reavy 1994; Holdsworth et al. 2015). In contrast to the aforementioned examples, the Orkney granite complex lacks steeply dipping fabrics commonly reported in proximity to subvertical strike slip faults. This likely reflects that a) the Orkney granite complex represents the central part of a larger pull-apart structure and hence is situated at some distance to the associated strike-slip faults, and b) the fabrics in the Orkney granite complex represent the youngest increment of strain (cf. Paterson et al. 1998), i.e. north-south extension, and do not preserve earlier magmatic fabrics reflecting sub-vertical ascent.

Alternatively, the north-south extension could reflect lateral gravitational spreading as a result of over-thickening of the crust above the Caledonian convergent margin, and/or slab break-off below it. In the models of Neilson et al. (2009) and Miles et al. (2016), slab break-off was initiated at the onset of continent-continent collision at ca. 430 Ma, leading to uplift, heating of the crust, magmatism and potentially gravitational spreading. Though Caledonian north-south striking extensional mineral lineations have been reported from the Glenfinnan and Loch Eil groups (Holdsworth and Roberts 1984), and the Loch Coire migmatite complex (Kinny et al. 1999; Kocks et al. 2006), these have been shown to reflect the Grampian phase of the Caledonian orogen or Precambrian events. It seems likely that extensional north-south trending lineations of uncertain age overprinting a ≥470 Ma fabric in the Neoproterozoic Fort Augustus granite gneiss also reflect Grampian deformation (Rogers et al. 2001). Thus, gravity spreading on Orkney at 430 Ma would appear to represent an anomalous, highly localized event. Furthermore, it is uncertain whether a crustal thickness gradient strong enough to drive gravitational collapse of the orogen was present already at the initiation of continent-continent collision at 432-430 Ma (cf. Viti et al. 2006).

Based on the scarce field evidence available, we propose that some variation of the strike-slip related settings above account for the emplacement of the Orkney granite complex. A subsidiary Orkney Islands strike-slip fault could root in the Great Glen Fault to the south-east, or it could merge with a deeper thrust fault (the Moine thrust). In either case, the merging at depth with crustal scale faults would provide a pathway for magmas forming at depth.

Timing of strain partitioning and high Ba-Sr magmatism in the Scottish Scandian collision

In Wenlock times (433.4-427.4 Ma) the Southern Uplands accretionary prism was transformed into a south-east verging fold-and-thrust-belt (Stone et al. 1987), and a foreland basin was formed on the Lake District Terrane on the Avalonia side of the collisional zone (Kneller et al. 1993). Meanwhile in northern Scotland, 431-429 Ma thrusting took place on the Moine thrust (Goodenough et al. 2011). Miles et al. (2016) thus proposes that buoyancy resistance to subduction of Avalonia beneath the Grampian orogen started at ca. 430 Ma.

Given our interpretation of the structural setting of the Orkney granite complex, the new high precision age of the Orkney granite complex dates strike-slip faulting in northern Scotland to 432-429 Ma. We propose that the timing of all these events show that strain partitioning into orogen normal thrusting (such as the Moine thrust) and orogen parallel transcurrent faulting (such as the Great Glen Fault) was already taking place at 431 Ma. It was thus an immediate response to the attempted subduction of Avalonia in the Wenlock, and testifies to the obliquity of the initial collision. This is in accordance with suggestions by Stewart and Strachan (1999), but contradicts a sequential evolution from orthogonal thrusting to transcurrent faulting with a switch in strain regime at 425 Ma, as suggested by e.g. Kocks et al. (2013).

The Orkney granite complex also yields the hitherto oldest age for the Scottish high Ba-Sr granite magmatism (cf. Rogers and Dunning 1991; Stewart et al. 2001; Olivier et al. 2008; Holdsworth et al. 2015), apart from an 433.5 ± 1.8 Ma Re-Os age interpreted as a minimum age for the Ballachulish complex (Conliffe et al. 2010). The age of the Orkney granite complex thus constrains the onset of the tectonic process (-es) that led to the widespread production of high Ba-Sr magmas below the Scottish highlands, and suggests that this process is coeval with the onset of transpressional deformation in northern Scotland. This provides new constraints on large-scale models of the Scandian tectonomagmatic evolution, such as the slab-breakoff and delamination models proposed by Atherton and Ghani (2002), Neilson et al. (2009) and Miles et al. (2016).

Conclusions

The Orkney granite complex belongs to the Scottish Newer granite Argyll suite and was emplaced at 431.93 ± 0.46 and 430.26 ± 0.92 Ma, with a late-magmatic aplitic phase dated to 428.50 ± 0.31 Ma. The emplacement took place during north-south extension; field observations hints at an emplacement depth of ca. 4-12 km. We relate the synmagmatic extension to formation of a pull-apart along a strike-slip fault related to the Great Glen Fault. The transcurrent Great Glen Fault and the Moine thrust were thus active at the onset of subduction of Avalonia beneath the Laurentian (Grampian) margin, testifying to immediate strain partitioning and high Ba-Sr magmatism in response to the Scandian collision.

Acknowledgments

John F. Brown is thanked for valuable discussions, field introductions to the geology of Orkney, and the use of his unpublished geological map of Stromness. Gunborg Bye Fjeld is thanked for help in the laboratory. This paper builds on master thesis work done by Audun D. Bjerga in 2016. This study was financed by a start-up grant from Oslo University to the first author. The authors gratefully acknowledge the reviewers Rob Strachan and Andrew Milesfor their helpful comments.

References

Andersen, T.B., Jamtveit, B.V., Dewey, J.F. & Swensson, E. 1991. Subduction and eduction of continental crust: a major mechanism during continent–continent collision and extensional collapse, a model based on the south Norwegian Caledonides. Terra Nova 3, 303–310.

Arthur, M.J. 1982. Discussion on a tectonic model for the emplacement of the Main Donegal Granite, NW Ireland. Journal of the Geological Society, London 144, 201-203.

Atherton, M.P., Ghani, A.A. 2002. Slab breakoff: a model for Caledonian, Late Granite syncollisional magmatism in the orthotectonic (metamorphic) zone of Scotland and Donegal, Ireland. Lithos 62, 65–85.

Augland, L., Andresen, A., Corfu, F. 2010. Age, structural setting, and exhumation of the Liverpool Land eclogite terrane, East Greenland Caledonides. Lithosphere 2, 267-286.

Bird, P.C., Cartwright, J.A., Davies, T.L. 2014. Basement reactivation in the development of rift basins: an example of reactivated Caledonide structures in the West Orkney Basin. Journal of the Geological Society 172, 77-85. doi.org/10.1144/jgs2013-098

Bluck, B.J. 1983. Role of the Midland Valley of Scotland in the Caledonian orogeny. Transactions of The Royal Society of Edinburgh 74, 119-136.

Bowring, J.F., McLean, N.M., Bowring, S.A. 2011, Engineering cyber infrastructure for U-Pb geochronology: Tripoli and U-Pb_Redux: Geochememistry, Geophysics, Geosystems 12, Q0AA19.

Carr, M.J. 2002. IGPET for Windows. Terra Softa Inc., Somerset, NJ.

Cawood, P.A., Strachan, R.A., Merle, R.E., Millar, I.L., Loewy, S.L., Dalziel, I.W., Kinny, P.D., Jourdan, F., Nemchin, A.A., Connelly, J.N. 2015. Neoproterozoic to early Paleozoic extensional and compressional history of East Laurentian margin sequences: The Moine Supergroup, Scottish Caledonides. Bulletin 127, 349-371. doi.org/10.1130/B31068.1

Chauvet, A., Séranne, M. 1994. Extension-parallel folding in the Scandinavian Caledonides: implications for late-orogenic processes. Tectonophysics 238, 31-54.

Chew, D.M., Strachan, R.A. 2014. The Laurentian Caledonides of Scotland and Ireland. Geological Society, London, Special Publications 390, 45-91.

Cohen, K.M., Finney, S.C., Gibbard, P.L., Fan, J.X. 2013 (updated 2017). The ICS international chronostratigraphic chart. Episodes 36, 199-204.

Conliffe, J., Selby, D., Porter, S.J., Feely, M. 2010. Re–Os molybdenite dates from the Ballachulish and Kilmelford Igneous Complexes (Scottish Highlands): age constraints for late Caledonian magmatism. Journal of the Geological Society 167, 297-302.

Cox, K. G., Bell, J. D., Pankhurst, R. J. 1979. The Interpretation of Igneous Rocks. London. Allen & Unwin.

Crowley, J.L., Schoene, B. and Bowring, S.A., 2007. U-Pb dating of zircon in the Bishop Tuff at the millennial scale. Geology, 35(12), pp.1123-1126.

Dewey, J.F., Strachan, R.A. 2003. Changing Silurian–Devonian relative plate motion in the Caledonides: sinistral transpression to sinistral transtension. Journal of the Geological Society 160, 219-229.

Fettes, D.J. 1999. Orkney Islands. Scotland special sheet. Solid and drift geology 1:100 000. Keyworth, Nottingham, British Geological Survey.

Flinn, D. 1992. The history of the Walls Boundary fault, Shetland: the northward continuation of the Great Glen fault from Scotland. Journal of the Geological Society 149, 721-726.

Fossen, H. 2010. Extensional tectonics in the North Atlantic Caledonides: a regional view. Geological Society, London, Special Publications 335, 767-793.

Fowler, M.B., Henney, P.J. 1996. Mixed Caledonian appinite magmas: implications for lamprophyre fractionation and high Ba-Sr granite genesis. Contributions to Mineralogy and Petrology 126, 199-215.

Fowler, M.B., Kocks, H., Darbyshire, D.P.F. and Greenwood, P.B., 2008. Petrogenesis of high Ba–Sr plutons from the northern highlands Terrane of the British Caledonian Province. Lithos, 105(1-2), pp.129-148.

Friedrich, A.M., Bowring, S.A., Martin, M.W., Hodges, K.V. 1999. Short-lived continental magmatic arc at Connemara, western Irish Caledonides: Implications for the age of the Grampian orogeny. Geology 27, 27-30.

Gapais, D. 1989, Shear structures within deformed granites: Mechanical and thermal indicators: Geology 17, 1144–1148. doi:10.1130/0091-7613(1989)017<1144:SSWDGM>2.3.CO;2.

Gates, A.E., Glover, L. 1989. Alleghanian tectono-thermal evolution of the dextral transcurrent Hylas zone, Virginia Piedmont, U.S.A. Journal of Structural Geology 11, 407–419. doi:10.1016/0191-8141(89)90018-7.

Goodenough, K.M., Millar, I., Strachan, R.A., Krabbendam, M., Evans, J.A. 2011. Timing of regional deformation and development of the Moine Thrust Zone in the Scottish Caledonides: constraints from the U–Pb geochronology of alkaline intrusions. Journal of the Geological Society 168, 99-114.

Gower, R.J., Simpson, C. 1992. Phase boundary mobility in naturally deformed, high-grade quartzofeldspathic rocks: evidence for diffusional creep. Journal of Structural Geology 14, 301-313.

Harland, W. B., Scott, R. A., Auckland, K. A., Snape, I. 1992. The Ny Friesland Orogen, Spitsbergen. Geological Magazine 129, 679–708.

Holdsworth, R.E. and Roberts, A.M., 1984. Early curvilinear fold structures and strain in the Moine of the Glen Garry region, Inverness-shire. Journal of the Geological Society 141, 327-338.

Holdsworth, R.E., Alsop, G.I., Strachan, R.A. 2007. Tectonic stratigraphy and structural continuity of the northernmost Moine Thrust Zone and Moine Nappe, Scottish Caledonides. Geological Society, London, Special Publications 272, 121-142.

Holdsworth, R.E., Dempsey, E., Selby, D., Darling, J.R.,. Feely, M.,. Costanzo, A., Strachan, R.A., Waters, P. , Finlay A.J., Porter, S.J. 2015. Silurian–Devonian magmatism, mineralization, regional exhumation and brittle strike-slip deformation along the Loch Shin Line, NW Scotland. Journal of the Geological Society 172, 748-762. doi.org/10.1144/jgs2015-058

Hutton, D.H.W. 1982. A tectonic model for the emplacement of the Main Donegal Granite, NW Ireland. Journal of the Geological Society 139, 615-631.

Jacques, J.M., Reavy, R.J. 1994. Caledonian plutonism and major lineaments in the SW Scottish Highlands. Journal of the Geological Society 151, 955-969.

Jaffey, A., Flynn, K., Glendenin, L., Bentley, W., Essling, A. 1971. Precision measurement of half-lives and specific activities of 235U and 238U. Physics Reviews C4, 1889-1906.

Kinny, P.D., Strachan, R.A., Friend, C.R.L., Kocks, H,, Rogers, G., Paterson, B.A. 2003. U–Pb geochronology of deformed metagranites in central Sutherland, Scotland: evidence for widespread late Silurian metamorphism and ductile deformation of the Moine Supergroup during the Caledonian orogeny. Journal of the Geological Society 160, 259-269. https://doi.org/10.1144/0016-764901-087

Kinny, P.D., Friend, C.R.L., Strachan, R.A., Watt, G.R. and Burns, I.M., 1999. U–Pb geochronology of regional migmatites in East Sutherland, Scotland: evidence for crustal melting during the Caledonian orogeny. Journal of the Geological Society, 156(6), pp.1143-1152.

Kirkland, C.L., Strachan, R.A., Prave, A.R. 2008. Detrital zircon signature of the Moine Supergroup, Scotland: contrasts and comparisons with other Neoproterozoic successions within the circum-North Atlantic region. Precambrian Research 163, 332-350.

Kneller, B.C., King, L.M., Bell, A.M. 1993. Foreland basin development and tectonics on the northwest margin of eastern Avalonia. Geological Magazine 130, 691–697.

Kocks, H., Strachan, R.A., Evans, J.A. 2006. Heterogeneous reworking of Grampian metamorphic complexes during Scandian thrusting in the Scottish Caledonides: insights from the structural setting and U–Pb geochronology of the Strath Halladale Granite. Journal of the Geological Society 163, 525-538. doi.org/10.1144/0016-764905-008

Kocks, H., Strachan, R.A., Evans, J.A., Fowler, M. 2013. Contrasting magma emplacement mechanisms within the Rogart igneous complex, NW Scotland, record the switch from regional contraction to strike-slip during the Caledonian orogeny. Geological Magazine 151, 899-915.

Krogh, T.E. 1982. Improved accuracy of U-Pb zircon ages by the creation of more concordant systems using an air abrasion technique: Geochimica et Cosmochimica Acta 46, 637–649, doi:10.1016/0016-7037(82)90165-X.

Lancaster, P.J., Strachan, R.A., Bullen, D., Fowler, M., Jaramillo, M., Saldarriaga, A.M. 2017. U–Pb zircon geochronology and geodynamic significance of 'Newer Granite'plutons in Shetland, northernmost Scottish Caledonides. Journal of the Geological Society 174, 486-497.

Law, R.D. Johnson, M.R.W. 2010. Microstructures and crystal fabrics of the Moine Thrust zone and Moine Nappe: history of research and changing tectonic interpretations. Geological Society, London, Special Publications 335, 443-503.

Leggett, J.K., McKerrow, W.T. Eales, M.H. 1979. The Southern Uplands of Scotland: a lower Palaeozoic accretionary prism. Journal of the Geological Society 136, 755-770.

Ludwig, K. 2003. ISOPLOT/Ex, A geochronological toolkit for Microsoft Excel. Berkeley Geochronology Center Special Publication 4, 70.

Lundmark, A.M., Sæther, T., Sørlie, R. 2014. Ordovician to Silurian magmatism on the Utsira High, North Sea: implications for correlations between the onshore and offshore Caledonides. Geological Society, London, Special Publications 390, 513-523.

Macdonald, R. and Fettes, D.J., 2006. The tectonomagmatic evolution of Scotland. Earth and Environmental Science Transactions of The Royal Society of Edinburgh, 97(3), pp.213-295.

Mattinson, J. 2005. Zircon U–Pb chemical abrasion ("CA-TIMS") method: Combined annealing and multi-step partial dissolution analysis for improved precision and accuracy of zircon ages. Chemical Geology 220, 47-66.

McBride, J.H., England, R.W. 1999. Window into the Caledonian orogen: Structure of the crust beneath the East Shetland platform, United Kingdom. Geological Society of America Bulletin 111, 1030-1041.

McDonough, W.F., Sun, S.S. 1995. The composition of the Earth. Chemical geology 120, 223-253.

McKerrow, W.S., Mac Niocaill, C., Dewey, J.F. 2000. The Caledonian orogeny redefined. Journal of the Geological Society 157, 1149-1154.

Miles, A.J., Woodcock, N.H., Hawkesworth, C.J. 2016. Tectonic controls on post-subduction granite genesis and emplacement: The late Caledonian suite of Britain and Ireland. Gondwana Research 39, 250-260.

Mykura, W., Flinn, D., May, F. 1976. British regional geology: Orkney and Shetland. Stationery Office Books (TSO).

Neilson, J.C., Kokelaar, B.P., Crowley, Q.G. 2009. Timing, relations and cause of plutonic and volcanic activity of the Siluro-Devonian post-collision magmatic episode in the Grampian Terrane, Scotland. Journal of the Geological Society 166, 545–561.

Oliver, G.J. 2001. Reconstruction of the Grampian episode in Scotland: its place in the Caledonian Orogeny. Tectonophysics 332, 23-49.

Oliver, G.J., Wilde, S.A., Wan, Y. 2008. Geochronology and geodynamics of Scottish granitoids from the late Neoproterozoic break-up of Rodinia to Palaeozoic collision. Journal of the Geological Society 165, 661-674.

Paterson, S.R., Fowler Jr, T.K., Schmidt, K.L., Yoshinobu, A.S., Yuan, E.S. and Miller, R.B., 1998. Interpreting magmatic fabric patterns in plutons. Lithos, 44(1-2), pp.53-82.

Read, H.H. 1961. Aspects of Caledonian magmatism in Britain. Liverpool and Manchester Geological Journal 2, 653–683.

Rey, P., Burg, J.P., Casey, M. 1997. The Scandinavian Caledonides aey etnd their relationship to the Variscan belt. Geological Society, London, Special Publications 121, 179-200.

Robinson, P., Tracy, R.J., Santallier, D.S., Andreasson, P.G., Gil-Ibarguchi, J.I. 1988. Scandian-Acadian-Caledonian sensu strictu metamorphism in the age range 430–360 Ma. Geological Society, London, Special Publications 38, 453-467.

Rogers, G., Dunning, G.R. 1991. Geochronology of appinitic and related granitic magmatism in the W Highlands of Scotland: constraints on the timing of transcurrent fault movement. Journal of the Geological Society 148, 17-27.

Rogers, G., Kinny, P.D., Strachan, R.A., Friend, C.R.L. and Paterson, B.A., 2001. U–Pb geochronology of the Fort Augustus granite gneiss: constraints on the timing of Neoproterozoic and Palaeozoic tectonothermal events in the NW Highlands of Scotland. Journal of the Geological Society 158, 7-14.

Schmitz, M., Schoene, B. 2007. Derivation of isotope ratios, errors, and error correlations for U-Pb geochronology using 205Pb-235U-(233U)-spiked isotope dilution thermal ionization mass spectrometric data. Geochemistry, Geophysics, Geosystems 8, Q08006.

Simpson, C., Wintsch, R.P. 1989. Evidence for deformation-induced K-feldspar replacement by myrmekite: Journal of Metamorphic Geology 7, 261–275. doi:10.1111/j.1525-1314.1989.tb00588.x.

Soper, N.J. 1988. Timing and geometry of collision, terrane accretion and sinistral strike-slip events in the British Caledonides. Geological Society, London, Special Publications 38, 481-492.

Soper, N.J., Woodcock, N.H. 1990. Silurian collision and sediment dispersal patterns in southern Britain. Geological Magazine 127, 527-542.

Soper, N.J., Strachan, R.A., Holdsworth, R.E., Gayer, R.A., Greiling, R.O. 1992. Sinistral transpression and the Silurian closure of Iapetus. Journal of the Geological Society 149, 871-880.

Soper, N.J., Ryan, P.D., Dewey, J.F. 1999. Age of the Grampian orogeny in Scotland and Ireland. Journal of the Geological Society 156, 1231-1236.

van Staal, C.R., Whalen, J.B., McNicoll, V.J., Pehrsson, S., Lissenberg, C.J., Zagorevski, A., Van Breemen, O., Jenner, G.A. 2007. The Notre Dame arc and the Taconic orogeny in Newfoundland. Geological Society of America Memoirs 200, 511-552.

van Staal, C.R. and Hatcher, R.D. 2010. Global setting of Ordovician orogenesis. Geological Society of America Special Papers 466, 1-11.

Steavenson, A.G. 1928. Some Geological Notes on Three Districts of Northern Scotland. Transactions of the Geological Society of Glasgow 18, 193-233.

Stephens, M.B., Gee, D.G. 1989. Terranes and polyphase accretionary history in the Scandinavian Caledonides. Geological Society of America Special Papers 230, 17-30.

Stephens, W.E., Halliday, A.N. 1984. Geochemical contrasts between late Caledonian granitoid plutons of northern, central and southern Scotland. Earth and Environmental Science Transactions of The Royal Society of Edinburgh 75, 259-273.

Stewart, M., Strachan, R.A., Holdsworth, R.E. 1999. Structure and early kinematic history of the Great Glen Fault Zone, Scotland. Tectonics 18, 326-342.

Stewart, M., Strachan, R.A., Martin, M.W., Holdsworth, R.E. 2001. Constraints on early sinistral displacements along the Great Glen Fault Zone, Scotland: structural setting, U - Pb geochronology and emplacement of the syn - tectonic Clunes tonalite. Journal of the Geological Society 158, 821-830.

Stewart, M., Strachan, R.A., Holdsworth, R.E. 1999. Structure and early kinematic history of the Great Glen Fault Zone, Scotland. Tectonics 18, 326-342.

Stone, P., Floyd, J.D., Barnes, R.P., Lintern, B.C. 1987. A sequential back-arc and foreland basin thrust duplex model for the Southern Uplands of Scotland. Journal of the Geological Society, London 144, 753-64.

Stone, P. 2014. The Southern Uplands Terrane in Scotland–a notional controversy revisited. Scottish Journal of Geology.

Stipp, M. 2002. The eastern Tonale fault zone: A ‘natural laboratory’ for crystal plastic deformation of quartz over a temperature range from 250 to 700°C: Journal of Structural Geology 24, 1861–1884. doi:10.1016/S0191-8141(02)00035-4.

Strachan, R.A. 2003. The metamorphic basement geology of Mainland Orkney and Graemsay. Scottish Journal of Geology 39, 145-149.

Streckeisen, A., 1974. Classification and nomenclature of plutonic rocks recommendations of the IUGS subcommission on the systematics of igneous rocks. Geologische Rundschau 63, 773-786.

Svensen, H., Hammer, Ø., Corfu, F. 2015. Astronomically forced cyclicity in the Upper Ordovician and U-Pb ages of interlayered tephra, Oslo Region, Norway. Palaeogeography Palaeoclimatology Palaeoecology 418, 150-159.

Tarney, J., Jones, C.E. 1994. Trace element geochemistry of orogenic igneous rocks and crustal growth models. Journal of the Geological Society 151, 855-868.

Torsvik, T.H., Rehnström, E.F. 2003. The Tornquist Sea and Baltica–Avalonia docking. Tectonophysics 362, 67–82.

Torsvik, T.H., Smethurst, M.A., Meert, J.G., Van der Voo, R., McKerrow, W.S., Brasier, M.D., Sturt, B.A., Walderhaug, H.J. 1996. Continental break-up and collision in the Neoproterozoic and Palaeozoic—a tale of Baltica and Laurentia. Earth-Science Reviews 40, 229-258.

Tribe, I.R., D'Lemos, R.S. 1996, Significance of a hiatus in down-temperature fabric development within syntectonic quartz diorite complexes, Channel Islands, UK: Journal of the Geological Society 153, 127–138. doi:10.1144/gsjgs.153.1.0127.

Viti, M., Albarello, D. and Mantovani, E., 2006. Quantitative insights into the role of gravitational collapse in major orogenic belts. Annals of Geophysics 49, 1289–1307.

Watson, J. 1984. The ending of the Caledonian orogeny in Scotland. Journal of the Geological Society, London 141, 193–214.

White, S. 1975. Tectonic deformation and recrystallisation of oligoclase. Contributions to Mineralogy and Petrology, 50, 287-304.

Wilson, G.V., Edwards, W., Knox, J., Jones, R.C.B., Stephens, J.V. 1935. The geology of the Orkneys. Memoirs of the Geological survey of Great Britain. HMSO, Edinburgh.

Figures, tables and captions.

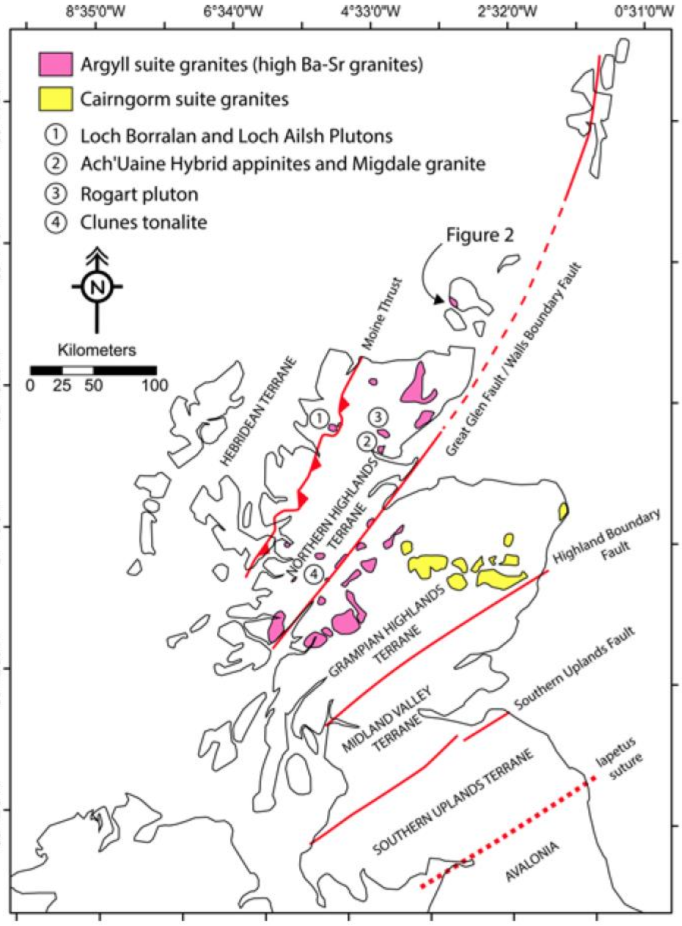

Fig. 1. Simplified regional map with selected high Ba-Sr and Cairngorm suite granitoids shown (after Stephens and Halliday 1984, via Macdonald and Fettes 2007; Fowler et al. 2008). The Orkney granite complex is shown as a high Ba-Sr granite (data from this study). Numbered localities are discussed in text.

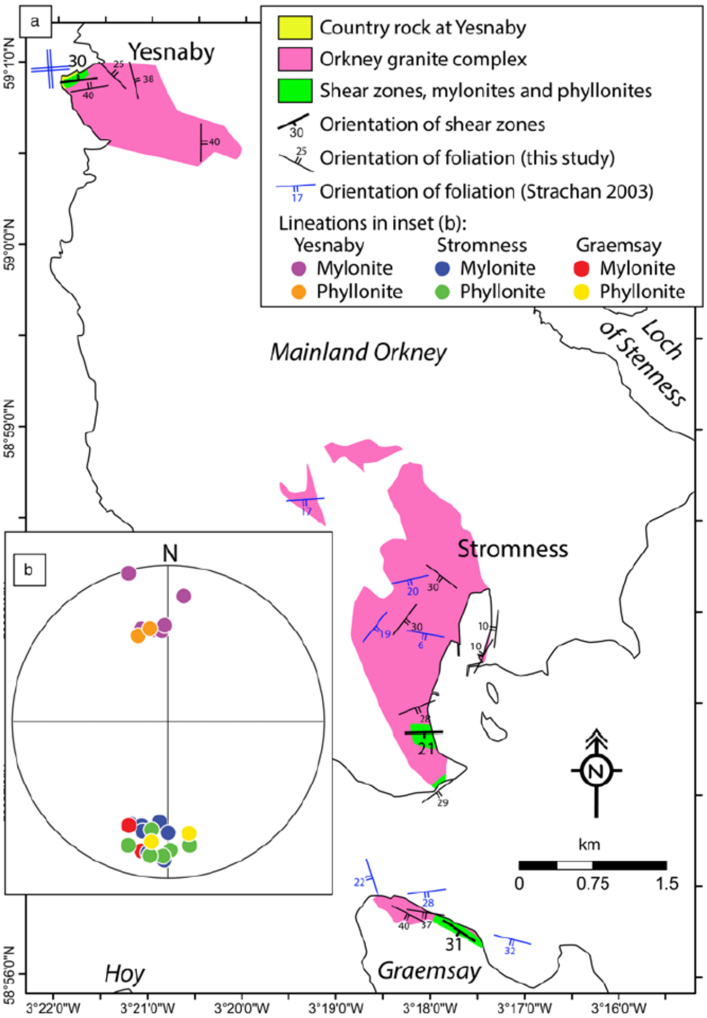

Fig. 2. The Orkney granite complex. (a) Sketch map of patchy exposures of the Orkney granite complex, modified from Fettes (1999). The complex presumably underlies the entire map area. Shear zones discussed in text (green) are exaggerated in size for visibility. (b) Inset shows mylonite and phyllonite lineations from the three main basement exposures on Orkney, Yesnaby, Stromness and Graemsay.

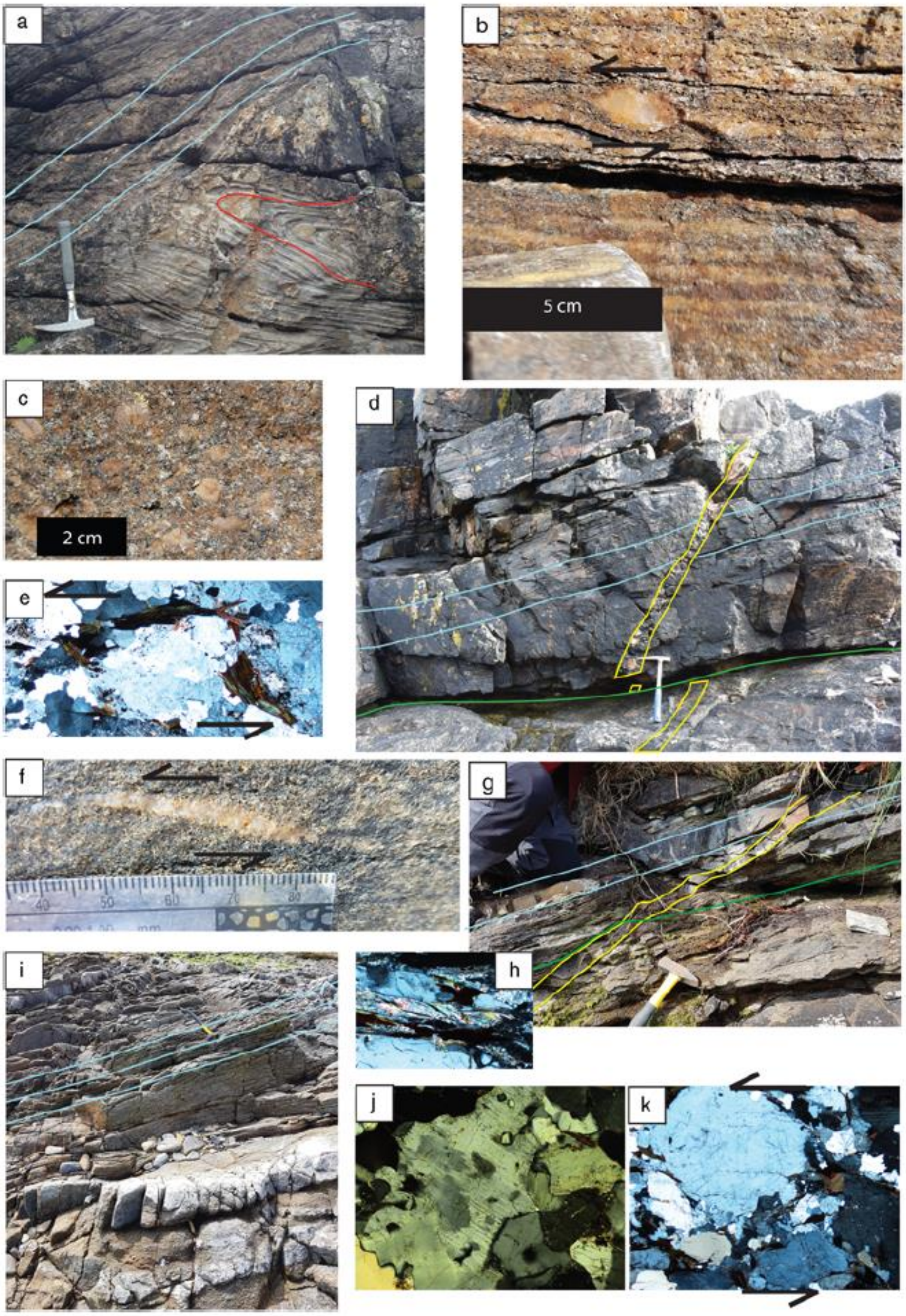

Fig. 3. Photographs and thin section images. (XP) = cross polarised light. (a) Isoclinally folded paragneiss (red) at Yesnaby cut at high angle by mylonite foliation (blue; 59°0’54.8’’N; 3°21’56.0’’W). Hammer for scale. View towards north. (b) Sigma porphyroclast in mylonitic granite at Yesnaby showing top-to-north sense of shear. View towards east. (c) Porphyric granite at Yesnaby developing into mylonite. View towards east. (d) Mylonite (blue) cut by aplite (yellow) at Yesnaby. The aplite is cut by a phyllonite zone (green). Hammer for scale. View towards south. (e) Thin section

image (XP) of mylonitic granite showing feldspar porphyroclast with core-mantle texture, surrounded by biotite. From Yesnaby. Shear sense is top-to-north. Width of view is 2.5 mm. (f) Top-to-north shear sense indicator in grey granite. View towards east. (g) Protomylonitic grey granite (blue) cut by aplite (ML17-15; yellow) that in turn is sheared and cut by phyllonite (green), but with minimal displacement. From Stromness (58°57'21.6"N; 3°18'2.0"W). Hammer for scale. View towards west. (h) Thin section image (XP) of phyllonite from Graemsay showing very fine grained muscovite fish and recrystallised and strained lensoid quartz. Width of view is 1.2 mm. (i) South-south-east-dipping protomylonitic foliation in grey granite along the shore south of Stromness (58°57'1.3"N; 3°17'58.4"W). Hammer for scale. View towards south-south-west. (j) Thin section image (XP) of plagioclase in partly mylonitic grey granite, Stromness. Note lobate grain boundaries between quartz and plagioclase and development of subgrains in the plagioclase. Width of view is 2.5 mm. (k) Thin section image (XP) of feldspar porphyroclast with core-mantle structure partly draped by biotite, from mylonitic granite at Stromness. Biotite is concentrated in S-planes and shear sense is top-to-south. Width of view is 2.5 mm.

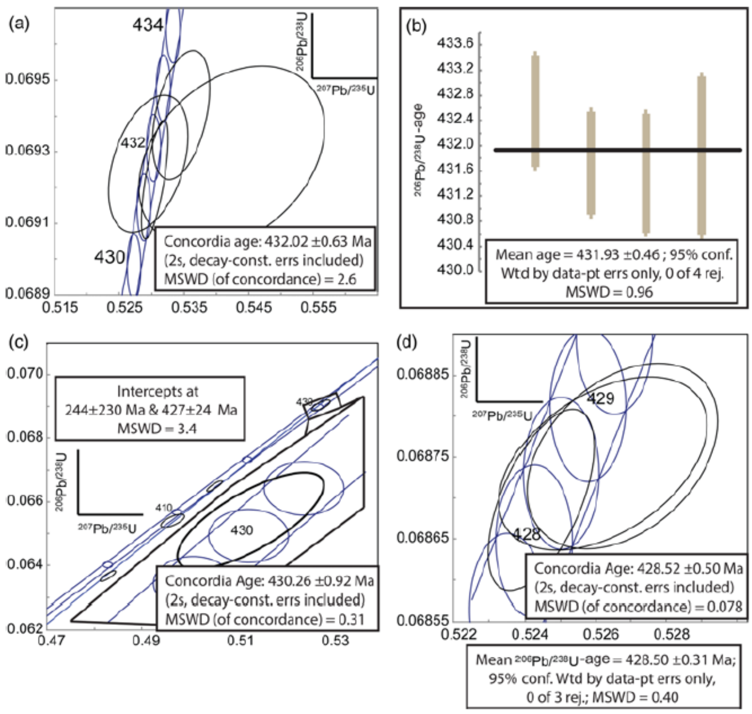

Fig. 4. Uranium-lead isotopic data. (a) Concordia diagram from AB 16-05. (b) Weighted average plot from AB 16-05. (c) Concordia plot from AB 16-04. Inset shows chemically abraded concordant zircon. d) Concordia plot from ML 17-15. All data points are plotted at the 2σ uncertainty level.

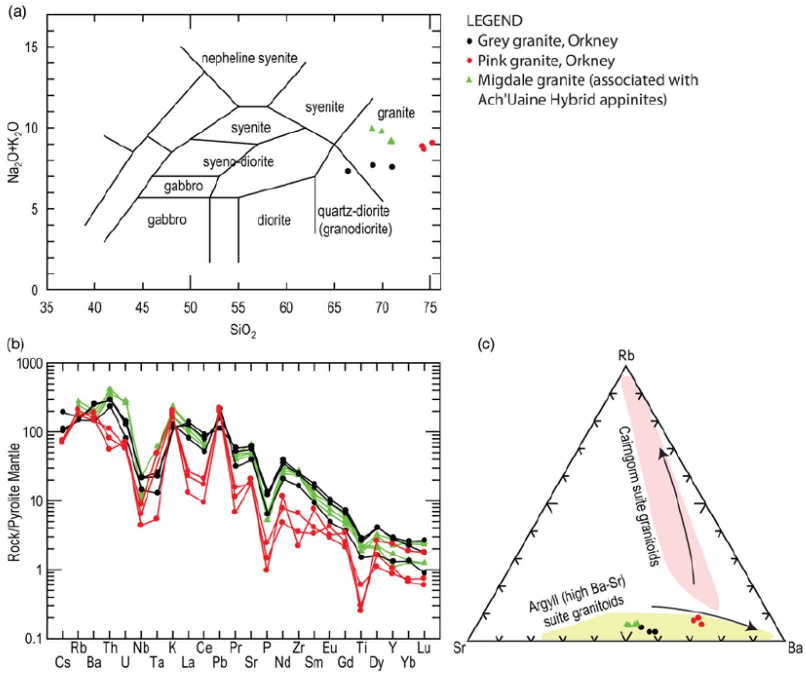

Fig. 5. Geochemical data (this study) and data from the Migdale granite for comparison (Fowler and Henney 1996). (a) Classification based on alkali-silica content after Cox et al. (1979). (b) Selected trace elements normalized to primordial mantle after McDonough and Sun (1995). (c) Ternary diagram for identification of high Ba-Sr granites. With increasing silica content the high Ba-Sr granites move towards higher relative Ba (yellow field), whereas the Cairngorm suite granites move towards higher relative Rb (pink field). The plots were made using IgPet (Carr 2002).

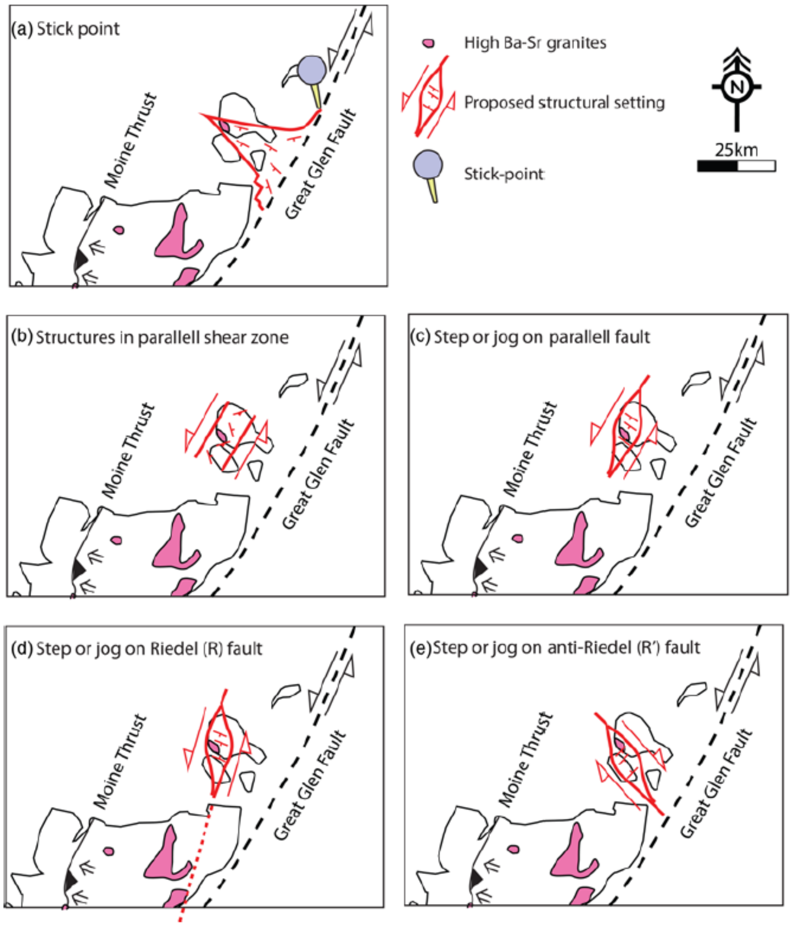

Fig. 6. Sketch models of some potential relations between extension on Orkney and strike-slip faulting at ca. 430 Ma. (a) Pull-apart due to stick point, i.e., a locked section of the fault, along the Great Glen Fault (or a subsidiary strike slip fault, not shown; e.g. Clunes; Stewart et al. 2001). (b) Extension in shear zone parallel to the Great Glen Fault. (c) Step or jog on fault parallel to the Great Glen Fault (e.g. Donegal pluton; Hutton 1982; Arthur 1982). (d) Step or jog on Riedel fault. (e) Step or jog on anti-Riedel fault (e.g. Rogart pluton; Kocks et al. 2013).

Table 1. *U-Pb isotopic data and ages*

Sample no. and position	Th/U*	Pb*/Pbc‡	Pbc (pg)‡	$^{206}Pb/^{204}Pb$‡	$^{207}Pb/^{206}Pb$§	% err‖	$^{207}Pb/^{235}U$§	% err‖	$^{206}Pb/^{238}U$§	% err‖	corr. coeff.	$^{207}Pb/^{206}Pb$¶	±‖	$^{207}Pb/^{235}U$¶	±‖	$^{206}Pb/^{238}U$¶	±‖	Discor-dance %
AB16-05 (58°57′20.5″N 3°18′01.4″W)																		
1	0.2	16	0.91	1039	0.05586	0.62	0.535	0.68	0.069403	0.21	0.419	447	14	433.2	2.4	432.56	0.89	3.2
2	0.2	2.2	2.2	163	0.0568	2.1	0.542	2.2	0.069284	0.30	0.327	483	46	440.0	7.7	431.8	1.3	10.6
3	1.0	6.0	2.7	338	0.05544	0.88	0.529	0.95	0.069267	0.23	0.403	430	20	431.4	3.3	431.74	0.94	−0.4
4	0.2	46	0.59	2896	0.055581	0.23	0.5305	0.32	0.069222	0.20	0.697	435.7	5.2	432.1	1.1	431.47	0.82	1.0
AB16-04 (58°57′20.5″N3°18′01.4″W)																		
1	0.4	70	0.89	4075	0.098364	0.12	2.6492	0.25	0.195334	0.20	0.878	1593.3	2.3	1309.5	1.9	1150.2	2.1	27.8
2	0.5	27	0.91	1569	0.07270	0.84	1.638	0.89	0.163374	0.31	0.327	1006	17	984.8	5.6	975.5	2.8	3.0
3	n.m	14	0.74	917	0.08535	0.45	1.8555	0.53	0.157667	0.23	0.533	1323.5	8.7	1065.4	3.5	943.8	2.0	28.7
4	0.3	19	4.6	1209	0.07942	0.89	1.463	0.91	0.133623	0.33	0.263	1183	17	915.4	5.5	808.5	2.5	31.6
5	n.m	25	4.6	1702	0.083508	0.38	1.5071	0.46	0.130895	0.28	0.575	1281.1	7.3	933.3	2.8	793.0	2.1	38.1
6	13	81	9.1	1277	0.055357	0.30	0.84831	0.39	0.111142	0.24	0.657	426.7	6.6	623.7	1.8	679.4	1.6	−59.2
7	0.3	83	0.90	5010	0.064589	0.14	0.76449	0.27	0.085844	0.21	0.855	761.0	2.9	576.6	1.2	530.9	1.1	30.2
8	0.1	48	0.67	3196	0.055461	0.21	0.5279	0.31	0.069032	0.20	0.737	430.9	4.7	430.4	1.1	430.32	0.83	0.1
9	0.0	16	26	1085	0.055125	0.14	0.50540	0.27	0.066494	0.21	0.874	417.3	3.0	415.4	0.9	415.00	0.85	0.6
10	0.1	5.5	240	386	0.055069	0.30	0.49660	0.41	0.065402	0.25	0.693	415.0	6.6	409.4	1.4	408.4	1.0	1.6
11	0.1	18	26	1182	0.055013	0.15	0.48286	0.28	0.063658	0.21	0.851	412.8	3.4	400.0	0.9	397.83	0.82	3.6
ML17-15 (58°57′22.1″N3°08′01.9″W)																		
1	0.4	2.1	2.0	144	0.0690	1.6	1.283	1.7	0.134742	0.27	0.365	900	33	838.0	9.7	814.9	2.0	9.5
2	3.2	6.9	0.63	257	0.0635	2.5	1.025	2.7	0.11714	0.52	0.382	724	54	716	14	714.1	3.5	1.4
3	0.4	13	0.64	827	0.06464	0.50	1.0098	0.53	0.113311	0.14	0.345	762	11	708.8	2.7	691.95	0.93	9.2
4	0.1	10	1.8	682	0.05557	0.39	0.52675	0.42	0.068752	0.13	0.377	435.1	8.6	429.6	1.5	428.63	0.56	1.5
5	0.1	11	1.5	743	0.05552	0.42	0.52622	0.46	0.068742	0.13	0.445	433.2	9.2	427.7	1.6	428.57	0.52	1.1
6	0.1	48	0.59	3189	0.05537	0.19	0.52447	0.23	0.068698	0.13	0.591	427.2	4.2	428.1	0.8	428.31	0.54	−0.3

Abbreviations: An. no., analysis number; n.m., not measured.*Model Th/U ratio calculated from radiogenic $^{208}Pb/^{206}Pb$ ratio and $^{207}Pb/^{235}U$ age.
†Pb* and Pbc represent radiogenic and common Pb, respectively; mol% ^{206}Pb* with respect to radiogenic, blank and initial common Pb.
‡Measured ratio corrected for spike and fractionation only.
§Corrected for fractionation, spike, and common Pb; up to 1 pg of common Pb was assumed to be procedural blank: $^{206}Pb/^{204}Pb = 18.04 \pm 0.40\%$; $^{207}Pb/^{204}Pb = 15.22 \pm 0.3\%$; $^{208}Pb/^{204}Pb = 36.67 \pm 0.5\%$ (all uncertainties 1-sigma). Excess over blank was assigned to initial common Pb.
‖Errors are 2-sigma, propagated using the algorithms of Schmitz & Schoene (2007) and Crowley *et al.* (2007).
¶Calculations are based on the decay constants of Jaffey *et al.* (1971). $^{206}Pb/^{238}U$ and $^{207}Pb/^{206}Pb$ ages corrected for initial disequilibrium in $^{230}Th/^{238}U$ using Th/U [magma] = 3.

Table 1. U-Pb isotopic data and ages.

Table 2. *Whole-rock geochemical analyses of grey and pink granite.* $Fe_2O_3^{(T)}$ *= total Fe expressed as* Fe_2O_3*. Samples no. 4, 5 and 29 were collected in Stromness, no. 7, 9 and 11 were collected at Yesnaby.*

Sample no:	AB16-05	AB16-29	AB16-07	AB16-11	AB16-09	AB16-04
Description:	grey granite	grey granite	grey granite	pink granite	pink granite	pink granite
Major elements (wt%)						
SiO_2	66.5	69.1	71.1	74.2	74.4	75.3
Al_2O_3	16.25	16.2	14.65	13.9	14.3	14.5
$Fe_2O_3^{(T)}$	3.3	3.28	1.89	0.6	1.33	1.16
CaO	3.28	2.38	1.78	1.04	0.84	1
MgO	1.1	1.04	0.38	0.07	0.08	0.09
Na_2O	4.57	4.74	4.46	3	3.76	3.66
K_2O	2.73	2.92	3.09	5.85	4.89	5.39
Cr_2O_3	<0.01	<0.01	<0.01	<0.01	<0.01	<0.01
TiO_2	0.48	0.44	0.25	0.05	0.12	0.06
MnO	0.04	0.04	0.02	0.01	0.01	0.01
P_2O_5	0.23	0.21	0.11	0.03	0.05	0.02
LOI	1.23	0.48	0.38	0.74	0.27	0.23
Total	99.97	101.09	98.27	99.64	100.24	101.56
Trace elements (ppm)						
Ag	<0.5	<0.5	<0.5	<0.5	<0.5	<0.5
As	<5	<5	<5	5	<5	<5
Cd	<0.5	<0.5	<0.5	<0.5	<0.5	<0.5
Co	7	6	2	1	2	2
Cu	8	8	3	5	3	7
Li	20	20	10	<10	<10	<10
Mo	1	<1	<1	<1	<1	1
Ni	7	5	1	1	<1	1
Pb	14	20	27	30	33	31
Sc	4	4	2	1	1	2
Tl	10	<10	<10	<10	<10	<10
Zn	68	68	43	6	20	16
Ba	1410	1380	808	1035	1260	964
Ce	127.5	110	72	15.7	28.7	34.9
Cr	20	20	10	10	10	20
Cs	3.42	1.8	1.96	1.58	1.46	1.57
Dy	2.3	2.28	0.91	1.76	0.74	1.09
Er	1.02	1.01	0.4	0.87	0.31	0.37
Eu	1.34	1.18	0.63	0.65	0.45	0.49
Ga	21.4	21.2	20.4	21.5	18.7	17.1
Gd	3.29	2.97	1.64	1.36	1.15	1.86
Hf	5.1	5.3	3.9	1.8	2.6	1
Ho	0.37	0.42	0.15	0.34	0.12	0.17
La	76	68.2	43.9	8.5	14.8	17.4
Lu	0.1	0.15	0.05	0.12	0.05	0.04
Nb	12	11.8	7.9	2.9	4.2	5.8
Nd	40.9	36.6	21.7	6	9.7	14.5
Pr	12.45	11.1	6.73	1.72	2.89	3.95
Rb	81.5	77.1	74.8	125.5	106.5	104.5
Sm	5.92	5.18	3.15	1.35	1.66	3.08
Sn	2	2	1	1	1	1
Sr	1030	932	654	345	410	355
Ta	0.8	0.7	0.4	0.2	<0.1	1.8
Tb	0.42	0.45	0.21	0.28	0.18	0.28
Th	19.15	19.4	15.5	4.4	6.45	8.78
Tm	0.12	0.15	0.07	0.13	0.04	0.05
U	2.19	2.41	1.37	1.44	1.17	1.27
V	46	40	21	8	8	7
W	1	2	1	1	1	1
Y	10.1	10.5	4.7	10.1	3.7	4.5
Yb	0.82	0.95	0.49	0.82	0.32	0.29
Zr	223	211	144	37	69	23

LOI, loss on ignition.

Table 2. Whole-rock geochemical analyses of grey and pink granite. Fe2O3(T) = total Fw expressed as Fe2O3. Samples no. 4, 5 and 29 were collected in Stromness, no. 7, 9 and 11 were collected at Yesnaby.